High capacity of integrated crop-pasture systems to preserve old stable carbon evaluated in a 60-year-old experiment

Maximiliano González Sosa[1,2], Carlos A. Sierra[2], Juan A. Quincke[3], Walter E. Baethgen[4], Susan Trumbore[2], M. Virginia Pravia[5,2]

1 Universidad de la República, Facultad de Agronomía, Departamento de Suelos y Aguas, Montevideo, Uruguay.
2 Max Planck Institute for Biogeochemistry, Jena, Germany
3 Instituto Nacional de Investigación Agropecuaria, INIA - La Estanzuela, Colonia, Uruguay
4 International Research Institute for Climate and Society, The Earth Institute, Columbia University, New York, USA
5 Instituto Nacional de Investigación Agropecuaria, INIA – Treinta y Tres, Treinta y Tres, Uruguay

Correspondence to: Maximiliano González Sosa (mgonzalez@fagro.edu.uy)

Abstract. Integrated crop-pasture rotational systems can store larger amounts of soil organic carbon (SOC) than continuous grain cropping. The aim of this study was to identify if the main determinant for this difference may be the avoidance of old C losses in integrated systems, or the higher rate of new C incorporation associated with higher C input rates. We analyzed the evolution of SOC in two agricultural treatments of different intensity (continuous cropping and crop-pasture rotational system) in a 60-year experiment in Colonia, Uruguay. We incorporated this information into a process of building and parameterizing SOC compartmental dynamical models, including data from SOC physical fractionation (POM > 53 µm > MAOM), radiocarbon in bulk soil and CO_2 incubation efflux. This modeling process provided information about C outflow rates from pools of different stability, C stabilization dynamics, as well as the age distribution and transit times of C. The differences between the two agricultural systems were mainly determined by the dynamics of the stable pool (MAOM). The outflow rate from this compartment was between 3.62 and 5.10 times higher in continuous cropping than in the integrated system, varying according to the historical period of the experiment considered. The avoidance of old C losses in the integrated crop-pasture rotational system determined that only 8.8% of the MAOM C was incorporated during the experiment period (after 1963) and that more than 85% was older than 100 years old. Moreover, half of the C inputs to both agricultural systems leave the soil in approximately one year due to high decomposition rates of the POM pool. Our results show that the high capacity to preserve old C of integrated crop-pasture systems is the key for SOC preservation of this sustainable intensification strategy, while their high capacity to incorporate new C into the soil may play a second role.

1 Introduction

30 Soil organic carbon (SOC) is currently at the center of international debate as a relevant property of soils to address global issues such as food security and climate change (Lal, 2018, 2016). On the one hand, it is the primary indicator of soil quality, because of its direct relationship with the physical, chemical, and biological properties that determine soil fertility and productivity. On the other hand, soils contain approximately two times more C than the atmosphere (Jobbágy and Jackson, 2000; Janowiak et al., 2017), and therefore, slight increases in their storage have the potential to reduce atmospheric CO_2 levels

35 and contribute to the fight against climate change (Fargione et al., 2018).

There is a growing scientific consensus that the genesis of stabilized SOC compartments (i.e. carbon that persists for decades to centuries or even longer once added to soil) occurs through the association of microbially synthesized products with the mineral phase (Cotrufo et al., 2015, 2013; Kallenbach et al., 2016; Kleber et al., 2011). Results from different studies suggest that higher levels of microbial anabolic activity under more diverse plant communities with perennial components are

40 responsible for the formation of SOC at higher rates (Ma et al., 2018; Zhu et al., 2020), with a strong relationship between the production of microbial necromass and the formation of stable organic matter (Córdova et al., 2018; Zhu et al., 2020). These processes are particularly enhanced in soils such as Mollisols that, due to their fine textures, promote the stabilization of microbial derived C in association with the mineral phase (Cotrufo et al., 2013).

Continuous monoculture and intensive tillage are the main causes of the deterioration of soil properties and have been

45 responsible for the emission of large amounts of C into the atmosphere (Rui et al., 2022). Various management practices such as reduced tillage, crop diversification, and application of amendments, have proven to be effective in increasing the poorly transformed particulate fractions of organic matter. However, their effectiveness in generating more persistent SOC in association with the mineral phase has been debated (Ogle et al., 2012; Rui et al., 2022). Nevertheless, the incorporation of perennial pastures into agricultural rotations also has proven to be a sustainable intensification strategy (Baethgen et al., 2021;

50 Davis et al., 2012; Pravia et al., 2019). Plant covers such as perennial pastures, characterized by a high partitioning of C towards their root systems (and rhizodeposition), could constitute an important tool to increase soil C sequestration (Sokol and Bradford, 2019). For example, microbial anabolism processes would be maximized by the presence of living roots releasing organic products within the soil (Schmidt et al., 2011; Sokol and Bradford, 2019; Villarino et al., 2021). In this regard, a previous study shows that integrated crop-pasture systems are able to maintain high soil C stocks compared to grain cropping

55 systems (Baethgen et al., 2021), but the processes that determine this dynamic continue to be poorly understood.

The study of C isotopes, and particularly ^{14}C, is a useful tool to understand the dynamics of C exchange between terrestrial ecosystems and the atmosphere (Torn et al., 2009). Radiocarbon is a measure of the time elapsed since C was fixed from the atmosphere via photosynthesis, and therefore, is an extremely useful tool to estimate the cycling rates of different compartments of C in terrestrial ecosystems (Trumbore, 2009). In the particular case of SOC, which constantly receives new

60 C inputs via photosynthesis and loses it through decomposition, the ^{14}C isotopic signature of SOC reflects both the decomposition rate and the radioactive decay rate of this isotope (Trumbore, 2000). During the 1960s, nuclear weapons testing

doubled the $^{14}C/^{12}C$ ratio in the atmosphere. Then, an agreement between the global nuclear powers halted atmospheric testing, which determined the generation of a peak of ^{14}C atmospheric concentration that serves as an isotopic tracer to understand the dynamics of C exchange between different compartments, such as SOC and the atmosphere on time scales of years to decades

65   (Torn et al., 2009; Trumbore, 2009). Moreover, the comparison of radiocarbon data in SOC and in CO_2 derived from microbial respiration provides information about the possible C sources for heterotrophic respiration (Nowinski et al., 2010; Torn et al., 2013). This information is highly useful to identify whether C losses as oxidation derive from active compartments with signatures close to the input (i.e. that of the atmosphere at a certain point in time), or if, on the contrary, there is a significant contribution of C from compartments of old organic matter that are undergoing destabilization processes.

70   Although the effect of management on SOC stocks is a question that has received significant research effort, the effect of environmental triggers (i.e., climate, agronomic management) on the persistence of SOC is a fundamentally relevant aspect that began to be addressed only recently (Lehmann and Kleber, 2015; Schmidt et al., 2011; Sierra et al., 2018b). Based on information about C flows, stocks, and isotopic tracers such as radiocarbon, mathematical representations can be generated in the form of systems of differential equations that represent C dynamics in soil (Sierra et al., 2018a). Then, once the model

75   correctly represents the measured data, emergent properties of the system such as the age and transit time can be derived (Sierra et al., 2018b). The age of the system is defined as the age of the C atoms in the soil since the time they entered the system until the moment of observation, while the transit time refers to the time that elapses since each atom enters the system until it is released from it (Sierra et al., 2018b). These diagnostic characteristics allow for a global understanding of the system dynamics, emerging as integrating properties of all the processes represented in the model (Sierra et al., 2017), and can be used to identify

80   the effect of environmental or management changes on the stability of C in the system as a whole.

In this work, we seek to improve the understanding of the biogeochemical processes that determine the success of integrated crop-pasture rotational systems in terms of their carbon storage and sequestration capacity compared to continuous cropping systems. The general objective was to identify if integrated crop-pasture rotational systems can store larger amounts of SOC than continuous cropping agriculture because of the avoidance of old C losses or due to a higher rate of new C incorporation

85   associated with higher input rates to the system. For this purpose, we analyzed the evolution of SOC in two agricultural treatments of different intensity (continuous cropping and crop-pasture rotational system) in a 60-year experiment in Colonia, Uruguay. We incorporated this information, data from SOC physical fractionation, radiocarbon measurements in SOC and CO_2 incubation efflux into a process of building and parameterizing SOC compartmental dynamical models. These models allow the analysis of C flow over time through compartments of different cycling rates and can be interpreted as processes of

90   SOC (de)stabilization responsible for the observed differences between the analyzed systems. Finally, we used these models to derive the distribution of age and transit time of C in each agriculture system. To address the objective, we proposed four alternative hypotheses with regards to why the integrated crop-pasture rotational systems have a higher C storage compared to intensive agriculture: 1) large input rates that promote SOC stabilization processes that support a high SOC stock (MAOM accrual hypothesis); 2) large input rates that promote the accumulation of large stocks of poorly stabilized particulate C (POM

95 accrual hypothesis); 3) high persistence of very stabilized old SOC linked to low oxidation rates of passive SOC pools (MAOM
stability hypothesis); 4) a combination of the previous processes.

2 Materials and methods

2.1 Experimental site

In 1963, the National Institute of Agricultural Research of Uruguay (INIA) established a long-term agricultural experiment
100 (LTE) at La Estanzuela experimental station (Colonia, Uruguay; 34°20'33"S, 57°43'25"W), located at the center of the Río de
la Plata Grassland Ecoregion (Baeza et al., 2022). The site has a humid temperate climate, with an annual mean rainfall of
1126.65 (± 269.94) mm and an accumulated reference evapotranspiration of 1192.54 (± 74.30) mm over 53 years of
meteorological records. The annual average temperature is 16.88 °C, with monthly average maximum temperatures of 29.04
°C and 14.83 °C, and monthly average minimum temperatures of 17.83 °C and 6.24 °C in January and July, respectively. The
105 variations in temperature and evapotranspiration between winter and summer are significant, and there is a trend towards lower
average accumulated rainfall volumes during the winter (Fig. 1a). Rainfall is highly variable among years, but it does not show
any long-term trend (Fig. 1b). The climatic characteristics of the region allow the establishment of summer and winter crops,
and typical agricultural systems consist of four crops in three years (Baethgen et al., 2021).
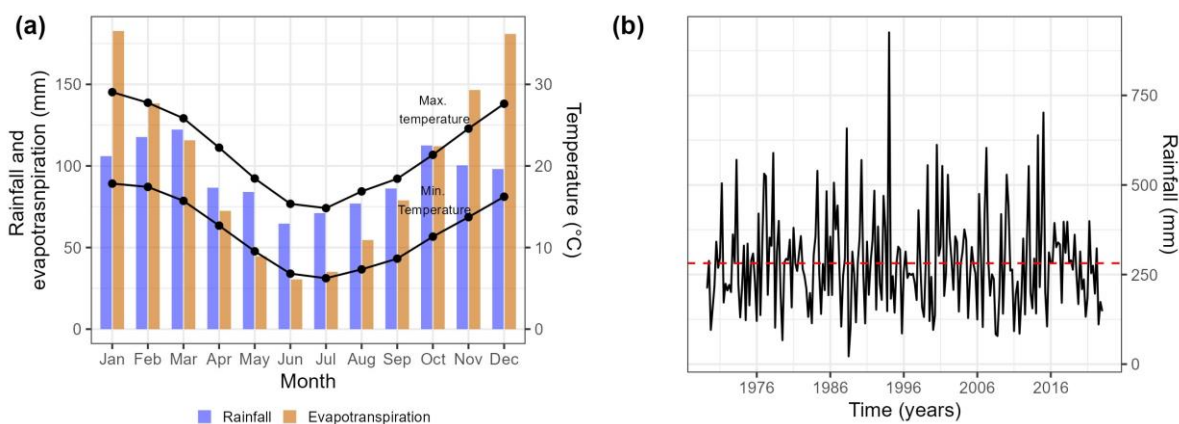
110

Figure 1. Monthly distribution of mean accumulated rainfall and evapotranspiration (left Y axis, bars) and monthly mean
maximum and minimum temperature (right Y axis, lines) (A); time series of seasonal accumulated rainfall (mm) (each value
corresponds to the accumulation of 3 consecutive months; dotted red line corresponds to the time series average) (B). The
information derives from a 53-year time series (1969 – 2022) provided by INIA's meteorological stations (INIA GRAS, 2023).

115

The geomorphology of the research site consists of rolling hills with an average slope of 3%. Soil is moderately acid with medium to high natural fertility and presents a well-developed Bt horizon and no rockiness. It is classified as a Haplic Phaeozem (Vertic, Eutric) in the FAO soil classification system (IUSS Working Group, 2014), and as a fine, smectitic Vertic

120 Argiudoll in the USDA Soil Taxonomy System (Soil Survey Staff, 2014). Detailed soil information from a historical sampling conducted at the experimental site is presented in Table 1.

Table 1. Soil characteristics of La Estanzuela LTE

Horizon	A_p	B_{t1}	B_{t2}	B_{t3}
Depth (cm)	0-30	30-42	42-72	72-97
Clay (g kg^{-1})	287	472	500	466
Silt (g kg^{-1})	637	466	461	486
Sand (g kg^{-1})	76	62	39	48
pH (H$_2$O)	5.6	6.1	6.6	6.8
pH (KCl)	5.6	5.6	5.2	5.5
SOC (g kg^{-1})	20.8	7.8	9.5	1.3
N_{tot} (g kg^{-1})	1.7	0.8	0.7	0.4
Ca (cmol$_c$ kg^{-1})	14.0	19.0	20.0	22.3
Mg (cmol$_c$ kg^{-1})	2.0	2.7	3.0	3.3
K (cmol$_c$ kg^{-1})	0.8	0.8	0.9	1.0
Na (cmol$_c$ kg^{-1})	0.3	0.4	0.5	0.5
CEC$_e$ (cmol$_c$ kg^{-1})	17.1	22.9	24.4	27.1
CEC$_{pH7}$ (cmol$_c$ kg^{-1})	20.6	25.5	26.6	28.4
Ef. Base Sat. (%)	100	100	100	100

Note: CECe: efective Cation Exchange Capacity; Ef. Base Sat: (Total Bases/CECe) * 100. Information obtained from a soil mapping conducted by the Uruguayan Ministry of Agriculture in 1985.

125

2.2 Long-term experiment

The INIA La Estanzuela LTE is one of the oldest agricultural experiments in the world. It was set up with the original objectives of evaluating the impact of N and P fertilization in continuous cropping systems, as well as the effect of incorporating pastures in rotation with crops as a N source and technological alternative to prevent soil quality loss (Díaz and Morón, 2003). The

130 LTE assesses the effect of seven treatments that represent a gradient of agricultural intensification on crop productivity, soil properties, and environmental impacts (Baethgen et al., 2021; Grahmann et al., 2020). This gradient ranges from continuous

cropping systems (with and without fertilizer application) to more conservationist agriculture in rotation with perennial pastures in different proportions of the rotation period.

The seven treatments are arranged in a randomized complete block design with three replications, and each of the 21 plots has an area of 0.5 ha. Currently, cropping sequences are not synchronized among the three replications of each treatment to have partial control of the year effect in the experimental design. Since 1963, the experiment has undergone a series of adjustments aimed at more accurately representing the evolution of Uruguayan production systems. These modifications involved minor changes in the crops included in each of the rotations and, mainly, changes in soil preparation systems with a trend towards no-tillage. In the first 20 years of the experiment, soil preparation was carried out with conventional tillage (moldboard and disk plow), which from 1983 was gradually replaced using chisel plow. From 2009 onwards, no-till farming was adopted in all treatments, eliminating the mechanical operations of soil preparation. Before the establishment of the LTE in 1963, the site had been cultivated for over 40 years, mainly with wheat (*Triticum aestivum* L.) – fallow systems. More detailed information about the LTE can be found in: Baethgen et al. (2021), Díaz and Morón (2003), Grahmann et al. (2020) and Quincke et al. (2019).

In order to maximize the differences in SOC stocks and dynamics, two contrasting treatments were selected: i) continuous agriculture with fertilizer application (CC) and ii) a crop-pasture rotation system with a 50% agricultural phase and 50% pasture phase (R). Currently, the CC system includes a sequence of barley (*Hordeum vulgare* L.) or wheat (*Triticum aestivum* L.) in winter alternating with corn (*Zea mays* L.), sorghum (*Sorghum bicolor* L. Moench), or soybean (*Glycine max* (L.) Merr.) in summer. The R system includes three years of the crop sequence from CC, rotating with three years of a perennial pasture that consists of a mixture of white clover (*Trifolium repens* L.), red clover (*Trifolium pratense* L.), birdsfoot trefoil (*Lotus corniculatus* L.) and tall fescue (*Festuca arundinacea* Schreb.). A detailed description of the crop sequences of these two production systems, as well as the modifications that occurred at different periods, can be seen in Fig. 2.

Winter crops (wheat, barley) were sown from May to June and generally harvested in December, while summer crops (sunflower, corn, sorghum, and soybean) were sown between November and December and harvested between April and May. The annual crops were harvested for grain production, while the plant residues were left on site. On the other hand, the pastures were mowed to simulate grazing, and the forage was left in the experiment.

Figure 2. Crop sequences of the CC and R treatments in the different historical periods of La Estanzuela LTE.

2.3 Soil Sampling and Analysis

All 21 plots were sampled annually to a depth of 20 cm from 1964 to 1996 and to a depth of 15 cm from that year onward. As outlined in a previous study conducted on this experiment (Grahmann et al., 2020), changes in the sampling depth are not expected to affect the results of long-term trends since the soil was systematically homogenized by tillage to a depth of 20 cm before sampling until 2009. Each composite sample consisted of 20 subsamples taken from the center of each plot. Samplings were performed during the fallow periods prior to the sowing of winter crops (April - May).

These samples were processed at the Laboratory of Water, Plants and Soils of INIA La Estanzuela Experimental Station (Colonia, Uruguay), with their C content determined using $K_2Cr_2O_7$ and heat with the method described by Tinsley (1950) until 2011, and by dry combustion at 900 °C followed by infrared detection from 2012 on a LECO analyzer (Wright and Bailey, 2001). The values obtained with LECO were adjusted by a coefficient of 0.81 to be comparable with the previous time series. This coefficient derived from an internal laboratory validation process in which a regression model was built with a large number of samples.

Additionally, a stratified sampling was carried out at 0-10 cm and 10-20 cm in 2008 and 2021. These samples were analyzed to obtain the radiocarbon signature in the bulk soil and in CO_2 efflux from incubations (only 2021 samples) at the Accelerator Mass Spectrometry (AMS) Laboratory at the Max Planck Institute for Biogeochemistry (MPI-BGC, Jena, Germany). We incubated the soil in hermetic glass bottles at 25 °C and with a moisture content equal to 60% of the soil field capacity to promote heterotrophic respiration. Air was extracted from each bottle once enough C had accumulated for graphitization and subsequent radiocarbon measurement (1.8 to 2.0 mg of C). To reach this threshold, the CO_2 concentration in the bottles was monitored with an infrared gas analyzer (Li-6262). Air extraction from the incubation bottles was carried out on a vacuum extraction line that allows the cryogenic purification of CO_2 from other gases (N_2, O_2, H_2O) (Trumbore et al., 2016a). Low vapor pressure gases (i.e., water) are trapped by passing the air flow through a trap submerged in a dry ice and alcohol bath (-78 °C). Then, the CO_2 is captured by making the air flow through a trap submerged in liquid nitrogen (-196 °C), while other gases (O_2, N_2) do not freeze at low pressures and are pumped away from the vacuum line (Trumbore et al., 2016a). Then, the purified CO_2 was reduced to graphite in the presence of H_2 as a reducing agent and iron powder (Fe) as a catalyst (Trumbore

185 et al., 2016a) at high temperature (> 500 °C). The mixture of graphite and iron was analyzed for its radiocarbon signature at the AMS facility of MPI-BGC.

Finally, the soil from the 2021 stratified sampling was physically fractionated by size to represent C pools with different cycling rates according to Cambardella and Elliot (1992), separating the particulate organic matter (POM, larger than 53 μm) from the mineral-associated organic matter (MAOM, less than 53 μm). These fractions were analyzed for C content by dry

190 combustion (Elementar Vario Max) at MPI-BGC. The weights of the recovered fractions and their C concentrations were used to determine the distribution of C among pools.

2.4 Monitoring of C inputs

The plots were sampled annually to obtain crop grain productivity as well as the annual dry matter aboveground productivity in the case of pastures. Based on this information, aboveground dry matter production of crops was estimated using harvest

195 indices extracted from Unkovich et al. (2010), Grant et al. (1999) and Mercau et al. (2007). Belowground C production was estimated considering aboveground production, shoot-to-root ratios (Bolinder et al., 2007) and net rhizodeposition to root biomass ratios (Pausch and Kuzyakov, 2018). For all crops and pastures, a C concentration of 0.45 g g (dry weight)$^{-1}$ for all plant parts was considered (Bolinder et al., 2007). Based on this information, soil C inputs were calculated as the sum of aboveground (subtracting grain production) and belowground C production for each period of the rotations. Accumulated

200 inputs for each period of the crop rotations were then annualized to obtain the mean C input for each rotation period. Subsequently, a global average for the entire historical series was obtained as the C inputs mean of all the periods for each system. All coefficients used in estimating soil C inputs are shown in Table 2.

Table 2. Coefficients used in calculations of soil C inputs based on crop and pasture yield data.

Crop	Species	Harvest index	Shoot/root ratio[4]	Net rhizodeposition/root biomass[5]
Wheat	*Triticum aestivum*	0.37[1]	7.4	0.54
Barley	*Hordeum vulgare*	0.38[1]	7.4	0.54
Sorghum	*Sorghum bicolor*	0.46[1]	5.6	0.54
Corn	*Zea mays*	0.49[1]	5.6	0.54
Sunflower	*Helianthus annuus*	0.4[1]	5.6	0.54
Flax	*Linum usitatissimum*	0.36[2]	7.4	0.54
Soybean	*Glicine max*	0.5[3]	5.2	0.54
Pastures			1.6	0.5

Note: [1] Unkovich et al., 2010, [2] Grant et al., 1999, [3] Mercau et al., 2007, [4] Bolinder et al., 2007, [5] Pausch and Kuzyakov, 2018.

2.5 Mathematical modelling

205 To analyze the systems as a whole and interpret the radiocarbon results concomitantly with all the available information, we used autonomous linear compartmental dynamic models with two pools of different decomposition rates and a transfer scheme between them (stabilization).

In the models, we assumed a horizon that represents the 0-20 cm layer of the experimental plots. C enters the system through a labile pool (representing POM C) and is then transferred to a stable pool (representing MAOM C) at a rate determined by

210 the cycling velocity of the labile pool and a C transfer coefficient between the two compartments.

The model is mathematically defined by a set of two differential equations, each of which describes the evolution of C stocks in each pool:

(1)

$$\frac{dC_l}{dt} = I - k_1 C_l$$

215
$$\frac{dC_s}{dt} = \alpha k_1 C_l - k_2 C_s$$

where I represents the amount of C inputs into the system; C_l is the amount of C stored in the labile pool (POM C); C_s is the amount of C in the stable pool (MAOM C); k_1 and k_2 are the output rates from the labile and stable pool, respectively; α is the C transfer coefficient, representing the proportion of carbon leaving the labile pool that is transferred to the stable pool (C stabilization).
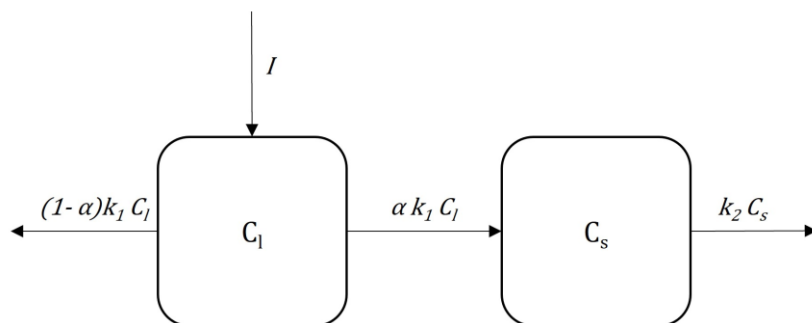
Figure 3. Graphical representation of the C compartmental model (Eq. 1) adjusted for CC and R agricultural systems.

The use of radiocarbon information as a tracer to improve the parameterization of this model is possible by the setup of a radiocarbon version of the model in Equation (1) that includes the rate of ^{14}C radioactive decay and the fraction of radiocarbon

225 in the atmosphere (Eq. 2).

(2)

$$\frac{dF_l C_l}{dt} = F_a I - k_1 F_l C_l - \lambda F_l C_l$$

$$\frac{dF_s C_s}{dt} = \alpha k_1 F_l C_l - k_2 F_s C_s - \lambda F_s C_s$$

where λ is the radiocarbon decay constant, Fa is the fraction of radiocarbon in atmospheric CO_2, F_l and F_s are the fractions of
230   radiocarbon in the labile and stable pool, respectively. Radiocarbon is expressed as absolute fraction modern, defined as the
absolute ratio of the sample to a standard (OX-I, oxalic acid made from a sugar beet crop of 1955), corrected for radioactive
decay to the year of measurement, and both corrected for mass-dependent isotope fractionation using $\delta^{13}C$ signature (Trumbore
et al., 2016b):

$$F = \frac{\left.\frac{^{14}C}{^{12}C}\right|_{sample,\,-25}}{0.95\,\left.\frac{^{14}C}{^{12}C}\right|_{OX,\,-19}\,e^{(y-1950)/8267}}$$

235   Fitting this model to the information from each of the agricultural systems (CC and R) allows testing the alternative stated
hypotheses. To achieve this, we will focus on evaluating the effect of the agricultural system on the C output rates of both
pools (k_1 and k_2) and the stabilization coefficient α. The time series of atmospheric radiocarbon data were obtained from
Reimer et al. (2013) and Hua et al. (2022) for the pre and post bomb period (southern hemisphere), respectively.

The time series of annual SOC monitoring (1964-2022), the proportion of C by fraction (POM - MAOM) in 2021, the
240   radiocarbon signature measurements in the bulk soil in 2008 and 2021, the radiocarbon signature in the CO_2 derived from
incubations in 2021, and C input data derived from the productivity monitoring of the plots (section 2.4) were used to
parameterize the model (Eq. 1 and Eq. 2) for each agricultural system (CC and R). The fitting was carried out to represent the
evolution of SOC stock in the POM and MAOM fraction as the labile (pool 1) and stable (pool 2) model compartments,
respectively.

245   Initially, an optimization procedure (Levenberg-Marquardt optimization algorithm) was applied to find the best set of
parameters that minimizes the differences between predictions and observations. Then, this set was used as a prior in a Bayesian
Markov Chain Monte Carlo (MCMC) procedure to estimate the probability density distribution of the parameters (Soetaert
and Petzoldt, 2010) and quantify the uncertainty associated with the generated models. Similar modeling approaches have
been used in studies such as Spohn et al. (2023), Crow et al. (2020), Crow et al. (2018), Sierra et al. (2013), Sierra et al.
250   (2012b). The R packages SoilR (Sierra et al., 2014, 2012a) and FME (Soetaert and Petzoldt, 2010) were used to implement
the models and parameterization procedures.

Based on the mathematical framework developed by Metzler and Sierra (2018), we conceptualized the deterministic models
proposed in Equation (1) and Equation (2) as their stochastic versions and calculated the probability distribution of the transit
time and the age of C in each of the systems and their pools. The age of C is a good indicator of the persistence of C in the
255   soil, while transit time is an indicator of the time during which a certain mass of C inputs will be retained by the system (Sierra
et al., 2018b).

The uncertainty of the fitted model for each agricultural system was propagated in a process whereby sets of parameters were
iteratively drawn from the distributions obtained through the Bayesian fitting procedure (MCMC). These sets were used to run
the models and calculate the ages and transit times in each iteration. By recording the values of these variables in each iteration

260   of the previous process, their distributions were constructed, capturing the variability transferred from the parameter
        populations.

2.6 Statistical analysis

        The effect of the agricultural system on the evolution of surface C stocks from 1964 onwards was analyzed using a mixed
265   linear model (LMM) ($p < 0.05$) with the agricultural system and time as fixed effect factors and the experiment plot as a
        random effect factor to represent the association of measurements made on the same plot in different years. This analysis was
        conducted using the lme4 package (Bates et al., 2015). The effect of the agricultural system on the stock of C in organic matter
        fractions (POM, MAOM), radiocarbon signature in the CO_2 efflux in 2021 and radiocarbon signatures in the bulk soil in 2008
        and 2021, were conducted with paired t-tests ($p < 0.05$). We tested the significance of the differences between the
270   compartmental model parameters and between the populations of ages and transit times through the comparison between
        agricultural systems of the 95% credible intervals for each of these variables (Makowski et al., 2019). All the analyses were
        performed in the R software (R Core Team, 2023).

3 Results

3.1 Measured data

        We found a statistically significant effect of the agricultural system and time factors on SOC down to 20 cm (Wald chi-square
        test, p value < 0.001). A sustained decline in SOC was observed in the CC system, decreasing from 52.6 ± 1.74 Mg ha^{-1} in
        1964 to 40.95 ± 3.89 Mg ha^{-1} in 2021 (Fig. 6a). In contrast, no trends of change were evident in the R system, where SOC has
280   fluctuated around 55 Mg ha^{-1} throughout the history of the experiment (Fig 5A). POM C stock showed significant differences
        between agricultural systems at all depths evaluated, whereas C stock in the MAOM fraction was significantly different in the
        0–10 cm layer and when considering the 0–20 cm layer as a whole, but not significantly different in the 10–20 cm layer
        individually (Table 3).

        Regarding the isotopic information, bulk soil radiocarbon was significantly different between systems in the 10–20 cm layer
285   and the 0–20 cm layer for both measurement years (2008 and 2021), showing a trend of difference in the 0–10 cm layer in the
        year 2008 (p value 0.077) and neither difference nor trend in this layer in 2021 (Table 3). It was observed that the soil at the
        evaluated depth is more depleted in radiocarbon in the CC system compared to the R system in both 2008 (CC $\Delta^{14}C_{0-20cm}$: -
        99.37 ± 17.24 ‰; R $\Delta^{14}C_{0-20cm}$: -40.0 ± 6.47 ‰) and 2021 (CC $\Delta^{14}C_{0-20cm}$: -72.11 ± 3.32 ‰; R $\Delta^{14}C_{0-20cm}$: -46.69 ± 6.65 ‰).
        CO_2 radiocarbon measured in soil incubation experiments from 2021 samples showed significant differences between systems
290   at all depths (Table 3), being more modern (closer to the isotopic signature of the atmosphere in 2021) in the case of the CC

system ($\Delta^{14}C_{0-20cm}$: 6.87± 3.09 ‰) than in the R system ($\Delta^{14}C_{0-20cm}$: 27.1 ± 4.82), which roughly resembles the atmospheric signature from the year 2014.

Table 3. Carbon stocks in fractions (POM, MAOM), radiocarbon in bulk soil and incubation efflux, and oxidation rates in incubations for each depth and agricultural system.

System	Depth (cm)	Bulk soil $\Delta^{14}C$ (‰)		Incubation efflux $\Delta^{14}C$ (‰)	Oxidation rate (mg C h^{-1})	POM stock (Mg ha^{-1})	MAOM stock (Mg ha^{-1})
		2008	2021	2021	2021	2021	2021
R	0 - 10	-34.17 [a] (3.57)	-47.27 [a] (9.54)	9.13 [a] (2.98)	0.0553 [a] (0.0029)	6.85 [a] (0.59)	23.3 [a] (0.26)
R	10 - 20	-46.9 [a] (9.9)	-45.97 [a] (2.97)	48.3 [a] (5.56)	0.0463 [a] (0.0033)	1.43 [a] (0.15)	20.8 [a] (0.36)
R	0 - 20	-40.0 [a] (6.47)	-46.69 [a] (6.65)	27.1 [a] (4.82)	0.051 [a] (0.0006)	8.28 [a] (0.71)	44.1 [a] (0.56)
CC	0 - 10	-91.5 [a] (17.60)	-60.4 [a] (3.71)	-6.5 [b] (3.15)	0.0407 [b] (0.041)	4.64 [b] (0.39)	19.0 [b] (0.91)
CC	10 - 20	-107.7 [b] (16.86)	-86.47 [b] (2.85)	25.63 [b] (3.77)	0.0287 [b] (0.029)	0.80 [b] (0.149)	18.40 [a] (1.13)
CC	0 - 20	-99.37 [b] (17.24)	-72.11 [b] (3.32)	6.87 [b] (3.09)	0.035 [b] (0.0021)	5.44 [b] (0.35)	37.4 [b] (1.66)

Note: Different letters within the same variable and depth indicate significant differences by paired t-test ($p < 0.05$) between systems. The value in parentheses indicates the standard error of the mean (n = 3).

The annual plant biomass production was calculated by considering both aboveground and root biomass (roots plus rhizodeposition) (Section 2.4). These quantities were transformed to C input rates considering a C concentration of 0.45 g g^{-1}, resulting in values of 2.87 ± 1.1 Mg ha^{-1} y^{-1} and 5.2 ± 1.2 Mg ha^{-1} y^{-1} for the CC system and R system, respectively.

3.2 Model results

Table 4 and Figure 4 show the results of the Bayesian calibration procedure (MCMC) for the model presented in Eq. 1 and Eq. 2 for each agricultural system, considering a surficial layer of 0-20 cm. To achieve a good model fit for the CC system, it was necessary to build a two-stage model because a higher rate of SOC loss was observed from 1964 to 1990 (Period 1) compared to 1991 to 2021 (Period 2). The parameters k_2 and α were allowed to be adjusted independently for each period. It was assumed that the parameter k_1 did not vary between the two periods. The R system was assumed to be in steady state with respect to SOC stocks, as no trends of change were observed in this variable over time.

Table 4. Summary information of the model parameters populations for each agricultural system (R and CC) obtained through the Bayesian fitting procedure (MCMC)

	R			CC				
	k_1	k_2	α	k_1	k_2 (P_1)	k_2 (P_2)	α (P_1)	α (P_2)
Mean	0.693	1.59E-03	1.48E-02	0.614	8.10E-03	5.75E-03	1.69E-02	2.34E-02
SD	0.018	4.39E-05	4.32E-04	0.089	1.41E-03	1.82E-03	1.72E-02	2.22E-02
Min	0.638	1.31E-03	1.20E-02	0.388	3.75E-03	1.75E-03	3.32E-05	4.17E-06
Max	0.860	1.80E-03	1.69E-02	1.344	1.41E-02	1.21E-02	7.97E-02	8.00E-02
Q1	0.680	1.57E-03	1.46E-02	0.553	7.12E-03	4.30E-03	4.51E-03	3.79E-03
Q2	0.692	1.59E-03	1.48E-02	0.604	7.89E-03	5.35E-03	1.10E-02	1.67E-02
Q3	0.705	1.61E-03	1.50E-02	0.661	8.88E-03	6.92E-03	2.35E-02	3.82E-02
LL	0.660	1.50E-03	1.39E-02	0.476	5.91E-03	3.19E-03	3.88E-04	3.36E-05
UL	0.727	1.67E-03	1.56E-02	0.804	1.14E-02	9.80E-03	6.70E-02	7.44E-02

Note: SD: standard deviation; Q1: first quartile; Q2: median; Q3: third quartile; LL: lower limit of 95% credible interval; UL: upper limit of 95% credible interval; k_1: POM pool decomposition rate; k_2: MAOM pool decomposition rate; α: transfer coefficient between pools; P_1: Period 1 of CC treatment; P_2: Period 2 of CC treatment.

310 Once the parameterization procedure reached convergence (25000 iterations), we observed that in both agricultural systems, the decomposition rate of the POM pool (k_1) was two orders of magnitude higher than that of the MAOM pool (k_2). No statistically significant differences were found in k_1 between agricultural systems (Fig. 4). However, a clear difference between agricultural systems was observed in the decomposition rate of the MAOM pool (k_2), which was approximately 5.10 times higher in Period 1 of the CC system compared to the R system, and 3.62 times higher in Period 2 of the CC system compared

315 to the R system. No significant differences were observed in the k_2 parameter between both periods of the CC system, although the mean and median values reached lower values in Period 2. There was also no significant difference in the transfer coefficient α between agricultural systems or between periods of the CC system. The mean values for α were very low in all cases, being $1.48 \pm 0.044\%$, $1.69 \pm 1.72\%$, and $2.34 \pm 2.22\%$ of the C outflow rate from the POM pool in the R system, Period 1 of the CC system, and Period 2 of the CC system, respectively.
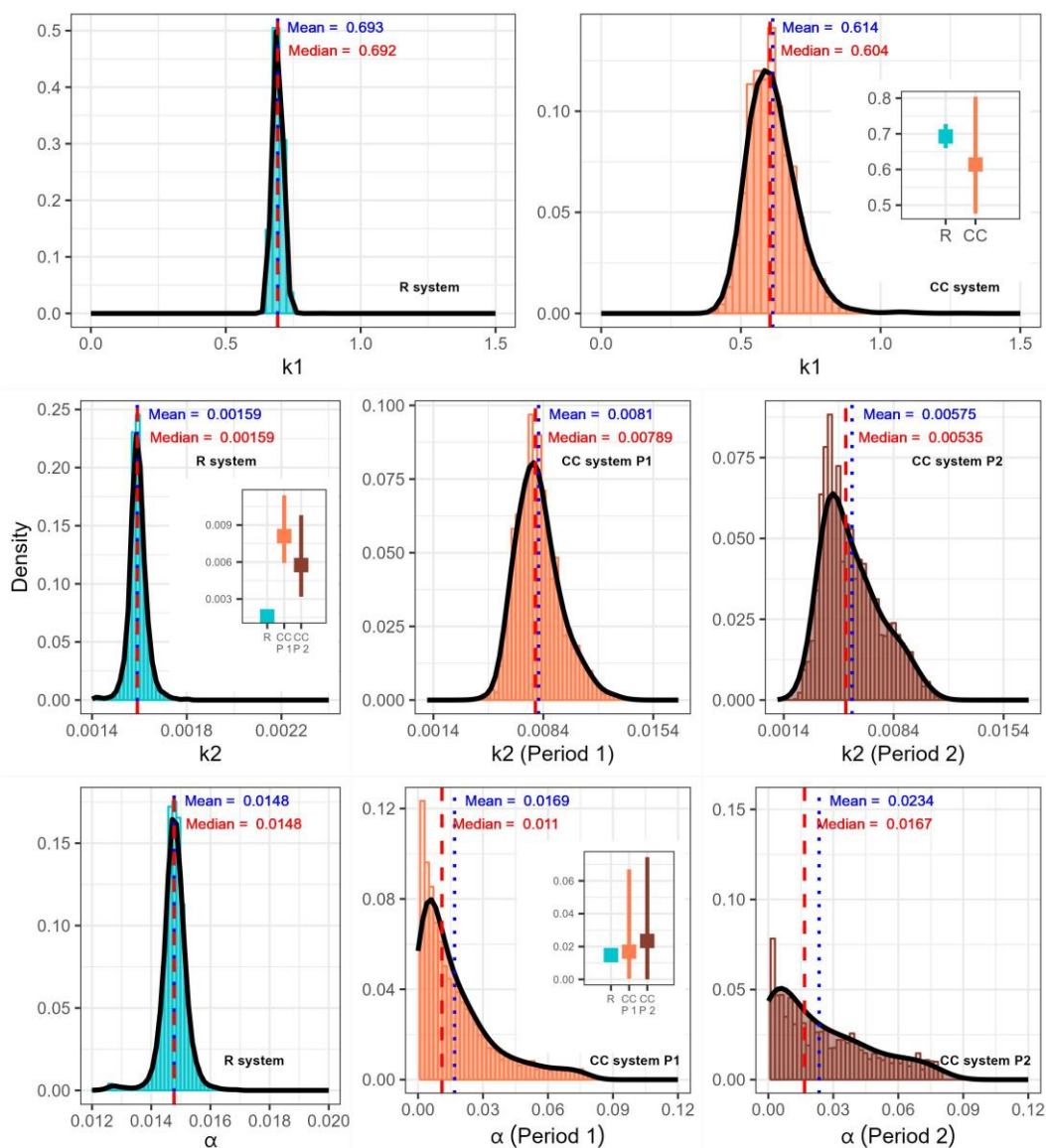
Figure 4. Compartmental model parameter populations for each agricultural system (R and CC) obtained through 25000 iterations of the Bayesian fitting procedure (MCMC) (0-20 cm). The inset graphs correspond to the comparison of the 95% credible intervals for each parameter between agricultural systems (the value of the parameter is represented in y axis).

325 Figures 5 and 6 display the fit to the measured data of the parameterized model for each agricultural system. In all cases, a relatively good agreement is observed between the observations and the estimates. In the case of the R system, the assumption of steady state for C stocks appears to be reasonable, as no significant trends of change over time in the measured values are

observed (Fig. 5a). The model is also able to represent in an excellent way the measured radiocarbon data in the soil and in the system's outflow (Fig. 5b).
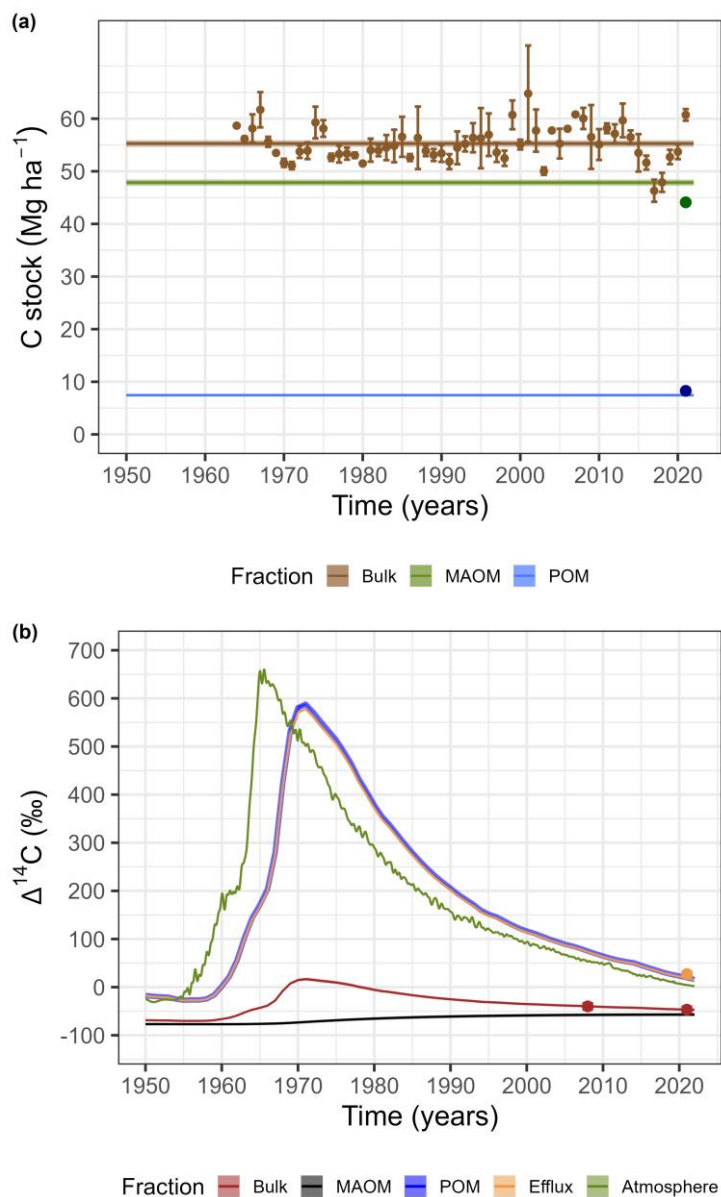
330

Figure 5. Model predictions of the temporal evolution of C stocks (0-20 cm) by fraction (A) and of the radiocarbon abundance (Δ^{14}C) since the bomb spike to the present for the integrated crop-pasture rotational system (R). Uncertainty ranges of model estimates obtained through sampling of the posterior parameter distribution (dark area: standard deviation; light area: 95% credible interval).
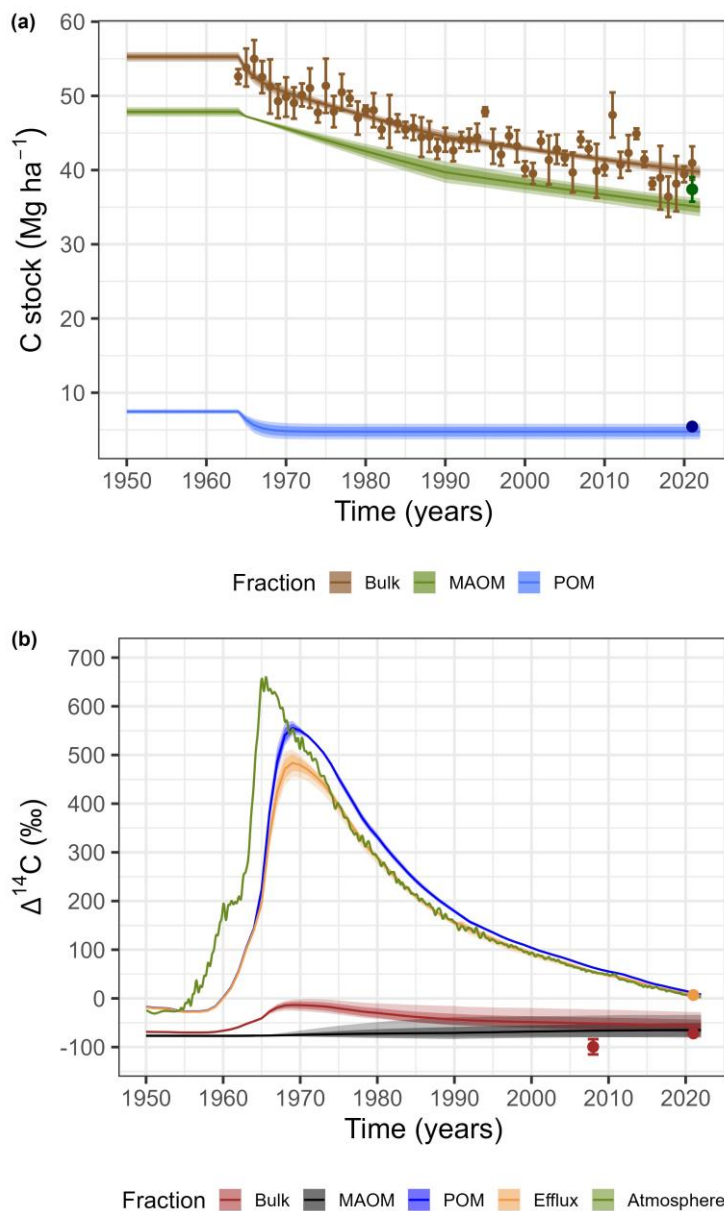
335

Figure 6. Model predictions of the temporal evolution of C stocks (0-20 cm) by fraction (A) and of the radiocarbon abundance ($\Delta^{14}C$) since the bomb spike to the present for the continuous cropping system (CC). Uncertainty ranges of model estimates obtained through sampling of the posterior parameter distribution (dark area: standard deviation; light area: 95% credible interval).

340

The main carbon flux rates for each agricultural system are presented in Table 5. It was assumed that the R system is in steady state with respect to SOC stocks, meaning that the total annual carbon outputs are equal to the inputs. For the CC system, the trajectory of carbon losses is determined by a higher rate of outputs than inputs. Additionally, the lower decomposition rate of

345   the MAOM pool in the R system resulted in this compartment having a lower relative importance in the total outputs (1.48%) compared to the CC system (6.3%). The stabilization flux (amount of carbon transferred from the POM pool to the MAOM pool per year) was 61.70% higher in the R system, which was primarily determined by the difference in input rates between the two systems, as the stabilization efficiency (Stabilization flux / inputs) was roughly the same in both agricultural systems.

350   **Table 5.** Main C flux rates derived from the compartmental model fitted to each agricultural system (for steady state condition for R system and for 2021 in CC system)

	R	CC
C input rate (Mg ha^{-1} y^{-1})	5.15 (1.2)	2.87 (1.1)
C total release (Mg ha^{-1} y^{-1})	5.15 (2.47E-05)	3.00 (2.1E-02)
POM C release (Mg ha^{-1} y^{-1})	5.08 (2.10E-03)	2.82 (6.20E-02)
MAOM C release (Mg ha^{-1} y^{-1})	0.076 (2.10E-03)	0.19 (6.20E-02)
Stabilization flux (Mg ha^{-1} y^{-1})	0.076 (2.20E-03)	0.047 (6.30E-02)
Stabilization efficiency (%)	1.48 (0.047)	1.75 (2.2)

Note: The value in parentheses indicates the standard deviation of the mean.

The mean system age, calculated under steady-state conditions, was found to differ between agricultural treatments, with

355   545.64 ± 17.61 years for the R system and 109.41 ± 74.39 years for the CC system (Fig. 7a). These ages are mainly determined by an older stable pool (MAOM) in the R system (mean age of 630.34 ± 17.70 years) compared to only 193.01 ± 59.00 years for CC system (Fig. 7c). Both the mean age of the system and the MAOM pool are significantly different between agricultural treatments, as no overlap of the credible intervals obtained through the propagation of the parameter distributions from the models is observed. The transit time distributions obtained for the two agricultural systems (Fig. 7d) show that the respired

360   carbon is predominantly of recent incorporation, with a mean transit time of 10.73 ± 0.38 and 6.15 ± 4.65 years in the R and CC systems, respectively. This relatively fast transit time is explained by a labile compartment (POM) with high decomposition rate and young mean ages (1.44 ± 0.037 years in the R system and 1.66 ± 0.22 years in the CC system) (Fig. 7b). Both the mean age of the POM pool and the mean transit time showed no significant differences between agricultural treatments. It is important to highlight that the age structure shown in this figure does not reflect the current condition of the CC system (which

365   is not in equilibrium yet) but rather the age distribution it will reach once it achieves steady state if its current dynamics are projected forward.
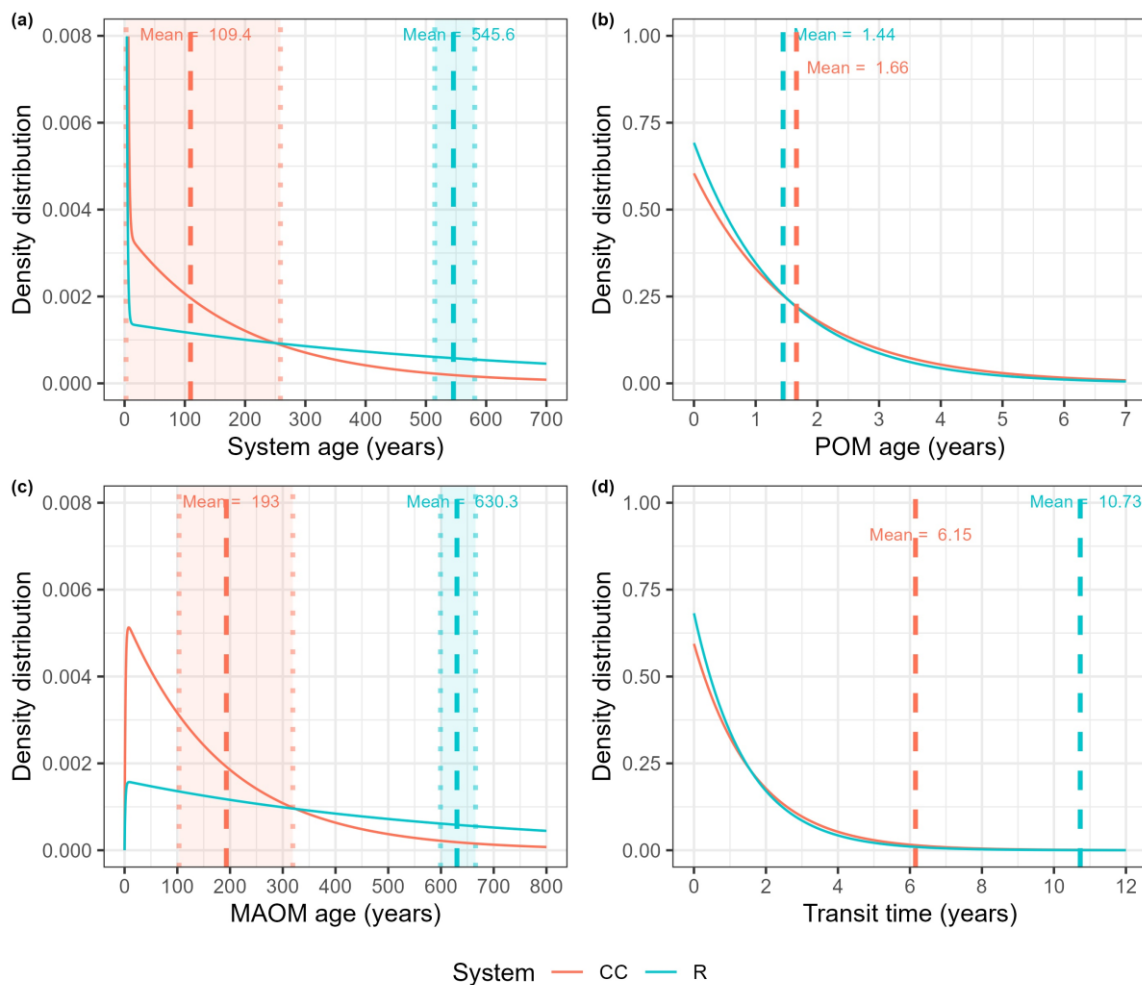
Figure 7. Distribution of C age in the system (A), in the POM pool (B), in the MAOM pool (C), and distribution of carbon
370   transit time in the system (D) for each agricultural treatment. Dashed vertical lines indicate the mean of the distribution, and
dotted vertical lines indicate the limits of the 95% credible interval of the mean (only intervals with significant differences
are shown). For the CC system, the distributions are those that will occur once the system reaches a steady state if its current
dynamics are projected forward.

375

4 Discussion

The integrative analysis conducted in this study, based on the parameterization of a compartmental model using monitoring
380   information of C stocks, productivity, and radiocarbon measurements in bulk soil and incubations, derived from a 60-year
agricultural experiment, allowed us to address the central research question concerning the processes responsible for higher C
stocks in integrated crop-pasture rotational systems compared to continuous cropping.

The model exhibited a good fit to the measured data in both agricultural systems, as shown in Figures 5 and 6, except for the
bulk soil radiocarbon in the CC system. Regarding this variable, while the model accurately represented the data for 2021, it
385   overestimated the value for 2008. This discrepancy could be attributed to the fact that this representation does not explicitly
characterize the soil erosion process, which might have displayed transient behaviors related to different soil preparation
methods over the different periods of the experiment. A previous study on the same experiment suggests that losses due to
erosion do not have a significant impact on the C balance in the systems analyzed (Baethgen et al., 2021). However, future
studies should consider this process, explicitly separating SOC losses and evaluating their impact on radiocarbon dynamics
390   and its use in model parameterization. Another possible explanation for the discrepancy between the CC system modeling and
the radiocarbon data measured in 2008 is a potential bias because the fractions measured in the laboratory (POM – MAOM)
may not exactly correspond to the kinetic pools defined in the model. This point could be tested in future studies with more
organic matter fractionation data distributed over time.

As demonstrated in other similar modeling approaches (Kätterer and Andrén, 1999; Sierra et al., 2013; Spohn et al., 2023;
395   Stoner et al., 2021), a two-pool structure proved to be adequate for representing these agricultural soil systems, characterized
by a dominant stable compartment (MAOM) with a decomposition rate two orders of magnitude lower than that of the labile
pool (POM) and a stabilization rate ranging between 1.48 to 2.34% of the C outflow from the labile pool (Fig. 4). This
mathematical representation of C dynamics accounts for the great difference between the radiocarbon signatures of bulk soil
and CO_2 in both agricultural systems. The former is highly negative and predominantly influenced by the signature of a
400   predominant stable pool that is relatively decoupled from the atmosphere, while the latter is very close to the atmospheric
signature and is predominantly explained by the decomposition of the labile pool at high rates.

Integrated crop-pasture systems are capable of achieving higher SOC stocks in the topsoil compared to continuous cropping,
as has been previously suggested (Baethgen et al., 2021; Pravia et al., 2019). The modeled SOC at steady state for the R system
was 55.27 ± 0.39 Mg ha^{-1} (Fig. 5a), whereas it was 39.74 ± 0.51 Mg ha^{-1} (Fig. 6a) in 2021 for the CC system. Subsequent
405   sections will discuss how different hypothesizes could account for the observed differences in SOC stock and dynamics.

POM Accrual Hypothesis

Concerning the poorly stabilized C, a modeled difference between agricultural systems in the C stock of the POM fraction for
2021 was found (2.68 Mg ha^{-1}), accounting for only 17.23% of the total SOC difference between the treatments (15.53 Mg ha^{-1}).
410   Therefore, the difference in SOC dynamics between the analyzed systems is not predominantly explained by the dynamics

of this fraction. Furthermore, no statistically significant difference was observed between the two agricultural systems in the outflow rate of this compartment (k_1) (Fig. 4), which was 0.693 ± 0.018 y^{-1} and 0.614 ± 0.089 y^{-1} for the R and CC systems, respectively. Hence, the observed POM C stock difference (R: 7.44 ± 0.19 Mg ha^{-1} and CC: 4.76 ± 0.65 Mg ha^{-1}) is explained by the different amount of material entering to each of the systems through the labile pool (R: 5.2 ± 1.2 Mg ha^{-1} y^{-1}; CC: 2.87

415 ± 1.1 Mg ha^{-1} y^{-1}), rather than by the dynamics of the compartment. Litter quality is a fundamentally important factor in determining the rates of C decomposition and stabilization under different management practices (Córdova et al., 2018). The two compared agricultural systems differ only in the plant species during the pasture phase of the R system, as the agricultural phase of this system is identical to the sequence of the CC system (Fig. 2). However, the mixture of species planted in the pasture phase (high-quality litter: red clover, white clover, birdsfoot trefoil; low-quality litter: fescue) could imply that the

420 intrinsic determinants of the C input concerning its susceptibility to decomposition do not vary significantly between treatments. The high outflow rates of this compartment indicates that the POM pool is responsible for most of the respiration flux in both systems (Table 5) as evidenced by the radiocarbon signature of the incubations (Table 3). Overall, higher inputs in the R system coupled with similar dynamics of the labile pools explain ~17% of the difference in carbon between R and CC systems.

425

MAOM Stability Hypothesis

In contrast to the POM pool, MAOM dynamics was strongly influenced by the agricultural treatment. The C outflow rate from the stable pool (k_2) was 5.10 times higher in Period 1 of the CC system compared to the R system, and 3.62 times higher in Period 2 of the CC system compared to the R system (Fig. 4), implying that MAOM stability has been the main factor

430 determining the observed differences between treatments. The difference between periods has been essentially caused by a much higher tillage intensity in the CC system, which promoted aggregate destabilization and increased soil aeration, exposing the C contained in the MAOM fraction to microbial degradation (Rui et al., 2022; Spohn and Giani, 2011). This process was particularly relevant in the first phase of the experiment (before 1984), characterized by conventional tillage application, with the CC system having twice as many tillage interventions as the R system. This is consistent with the steeper slope of SOC

435 loss observed until 1990 (Fig. 6a), determining a higher k_2 value in this period (Fig. 4, Table 4). However, it is striking that the k_2 coefficient was found to be 3.62 times higher in the CC system from 1990 onwards, when reduced tillage technologies had already started to be implemented, evolving into a no-till system in 2009.

New approaches to SOC dynamics suggest that MAOM destabilization processes also depend on the availability of nutrients for the microbial biomass. Lower levels of labile C in systems with fewer inputs and lower POM stocks may lead to an increase

440 in the destabilization of the MAOM pool, which would take on a role as a nutrient provider for microbial biomass (Daly et al., 2021). This may be one of the reasons why high relative rates of decomposition of the stable fraction are sustained even after the incorporation of minimum tillage and no-till systems. Additionally, Hall et al. (2019) suggest that the alternation in crop rotations of N-rich inputs like soybeans and other crops with high C/N ratio litter like that produced by crops such as wheat,

corn, or sorghum may enhance litter and stable SOC decomposition due to the priming effect generated by the high C/N litter,

445 accelerated by the elevated growth of microbial biomass previously caused by the N-rich soybean litter.

MAOM Accrual Hypothesis

The C flow to the MAOM pool (stabilization) emerged as a second key factor in determining the SOC differences between the treatments. In the mathematical representation used in this study (Eq. 1, Eq. 2, Fig. 3), this process is governed by the

450 coefficient α that represents the amount of C flowing to the stable pool per unit of C leaving the labile compartment, and k_1 (the rate at which material leaves the labile pool). Although these coefficients did not differ significantly between the two agricultural systems, the larger C stock in the POM pool led to a more intense C stabilization process in the R system, represented by a greater C flux to MAOM (R: 0.076 Mg ha^{-1} y^{-1}; CC: 0.047 Mg ha^{-1} y^{-1}) (Table 5).

Various studies agree that the processes of SOC stabilization in association with the mineral phase rely on a high level of

455 microbial activity, with subsequent anabolic production of organic compounds (Cotrufo et al., 2015, 2013; Kallenbach et al., 2016; Kleber et al., 2011), that flow to stable compartments mediated by the formation of microbial necromass (Córdova et al., 2018; Zhu et al., 2020). The observed results are consistent with the intensification of these processes in the R system due to a greater quantity of C inputs. However, this study did not find that these processes were altered by varying qualities of litter, as proposed in previous works (Ma et al., 2018; Zhu et al., 2020), given that no differences were observed in the

460 parameters regulating the dynamics of each unit mass of C entering the system (k_1 and α) (Fig. 4). The higher C stabilization process in integrated crop-pasture systems seems to be explained by the quantity rather than the quality of the inputs.

From a practical point of view, it is clear that the incorporation of no-tillage systems is fundamental for the conservation of stabilized SOC. In turn, the inclusion of pasture phases with perennial species and constant C inputs to the soil has an effect

465 of increasing the C stabilization rate, but primarily of reducing the losses of stabilized SOC. This would be related both to differences in the stoichiometry of the inputs and to the reduction of fallow periods between crops that favor microbial oxidation of SOC.

Global Properties (Transit Time and Age)

470 The model structure and its parameterization gave rise to emergent properties such as C transit time and age (Sierra et al., 2018b). The steady-state representation of the R system showed that, on average, each atom of C remains 10.73 years after entering the system (mean transit time) (Fig. 7d). However, the transit time distribution was strongly right-skewed, with half of the C entering this system remaining for only 1.02 years (median transit time). This value approximately matched the mean age of the POM pool (1.44 years) (Fig. 7b), making it clear that the system's outputs are predominantly explained by a labile

475 pool decomposing at high rates and very low outputs of old C from the MAOM pool (mean age 630.3 years) (Fig. 7c), which heavily skews the C outflow age distribution to the right (Fig. 7d).

Regarding the CC system, the age distribution of the POM pool did not differ from that of the R system (Fig. 7b), determining that half of the C entering this system remains for similar periods (median transit time 1.18 years). However, the mean transit time reached lower values (6.15 years) (though not significantly different from R) (Fig. 7d). This is explained by the different

480   dynamics of the stable pool, which, because of higher decomposition rates, tends to become younger as the new C entering this compartment is less diluted in a large stock of old C. This is consistent with the lower average ages of the MAOM pool (Fig. 7c) and the bulk soil in this system (Fig. 7a), and with the even more right-skewed distributions observed for CC system in steady-state condition compared to the R system. Analyzing the transit time results for both systems globally, we found them close to those observed at a long-term experiment in New Zealand with a similar climate (Stoner et al., 2021).

485   Focusing on the age structure of C in the R system, we found that 21.5% of its C was incorporated during the period of the experiment (59 years), of which more than half (13.5%) consists of POM C, a pool that in its entirety is younger than the age of the experiment. The remainder of the total renewed C is accounted for by MAOM, of which approximately 8.8% entered the system after the year 1963; therefore, most of this pool was already present in the soil before the experiment's installation. Analyzing the age structure of MAOM specifically, 85.4% is older than 100 years, 44.8% is older than 500 years, and 19.7%

490   is older than 1000 years. Conducting the same analysis for the CC system would be meaningless as it has not yet reached a steady state, a necessary assumption for calculating these properties (Manzoni et al., 2009; Sierra et al., 2021). For this reason, the distributions presented in Fig. 7 for the CC system do not represent the current age structures but rather those that will occur once the system reaches steady state if its current dynamics are projected forward. However, it is clear that the CC system induces a "rejuvenation" effect by significantly losing very old C from the stable pool.

495

5 Conclusions

Based on a modeling process that uses data from a 60-year monitoring experiment, as well as soil radiocarbon measurements from soil and incubations, we conclude that the greater SOC stock in integrated crop-pasture systems compared to conventional agricultural systems is primarily caused by the preservation of ancient carbon, because of lower oxidation rates of the stable

500   pool when compared to continuous cropping systems. The stability of MAOM in the integrated system leads to an extremely ancient age distribution, with only 8.8% of the carbon in this pool having entered the system since the experiment's initiation in 1963. Another important factor in determining the current difference in carbon stocks between the systems is the higher flow of carbon from the POM to the MAOM pool (stabilization). This process occurs to a greater extent in the integrated system due to higher carbon inputs and consequent greater microbial activity, rather than based on differences in the inherent

505   qualities of the input material.

Future work should consider the effects of soil erosion on radiocarbon dynamics and its implications in model's adjustment and interpretation. Additionally, the evaluation of integrated crop-pasture systems established on already-degraded soils that are on pathways to recovering carbon stocks should also be considered.

Funding statement

510 Funding for this work was provided by the cooperation project "Understanding how land management alters C and N cycling in Uruguayan agro-ecosystems" (ANII MPI_ID_2018_1_1008457) between the Instituto Nacional de Investigación Agropecuaria (INIA – Uruguay), the Agencia Nacional de Investigación e Innovación (ANII - Uruguay), and the Max Planck Institute for Biogeochemistry (MPI-BGC - Germany), under the collaboration agreement between INIA- Uruguay and the Max Planck Society (MPG -Germany). The first author received a fellowship from the Comisión Académica de Posgrado (CAP) of

515 the Universidad de la República (Uruguay) and an internship grant from the Comisión Sectorial de Investigación Científica (CSIC) of the Universidad de la República (Uruguay), which were fundamental for the development of this work.

Code and data availability

Code and data are available for review at the following git repository: https://github.com/maxigon-
520 23/data_and_code_gonzalez_23/tree/main/CODE_AND_DATA. It will be published with a DOI that can be cited in the publication.

Author contribution

Conceptualization: MGS, CAS, MVP. Data Curation: JAQ, MVP. Formal analysis: MGS. Funding acquisition: MVP.
525 Investigation: MGS. Supervision: MVP, CAS, JAQ, WEB, ST. Writing – original draft preparation: MGS. Writing – review and editing: MGS, MVP, CAS, JAQ, WEB, ST. All authors have read and agreed to the published version of the manuscript.

Competing interests

The authors declare that they have no conflict of interest.

530 **Acknowledgements**

The authors are grateful to Emiliano Barolín, Eduardo H. Vergara and Gualberto Soulier for their support during the sampling campaigns, as well as to the historical staff of INIA for their contribution to the development and maintenance of the long-term experiment. We would also like to thank Iris Kuhlmann, Axel Steinhof, and Andrés Tangarife-Escobar for their support in the laboratory activities at MPI-BGC that contributed to the data acquisition for this work.

References

Baethgen, W. E., Parton, W. J., Rubio, V., Kelly, R. H., and M. Lutz, S.: Ecosystem dynamics of crop–pasture rotations in a fifty-year field experiment in southern South America: Century model and field results, Soil Sci. Soc. Am. j., 85, 423–437, https://doi.org/10.1002/saj2.20204, 2021.

Baeza, S., Vélez-Martin, E., De Abelleyra, D., Banchero, S., Gallego, F., Schirmbeck, J., Veron, S., Vallejos, M., Weber, E., Oyarzabal, M., Barbieri, A., Petek, M., Guerra Lara, M., Sarrailhé, S. S., Baldi, G., Bagnato, C., Bruzzone, L., Ramos, S., and Hasenack, H.: Two decades of land cover mapping in the Río de la Plata grassland region: The MapBiomas Pampa initiative, RSASE, 28, 100834, https://doi.org/10.1016/j.rsase.2022.100834, 2022.

Bates, D., Mächler, M., Bolker, B., and Walker, S.: Fitting Linear Mixed-Effects Models Using lme4, J. Stat. Soft., 67, https://doi.org/10.18637/jss.v067.i01, 2015.

Bolinder, M. A., Janzen, H. H., Gregorich, E. G., Angers, D. A., and VandenBygaart, A. J.: An approach for estimating net primary productivity and annual carbon inputs to soil for common agricultural crops in Canada, Agric Ecosyst Environ, 118, 29–42, https://doi.org/10.1016/j.agee.2006.05.013, 2007.

Cambardella, C. A. and Elliott, E. T.: Particulate soil organic-matter changes across a grassland cultivation sequence, Soil Sci. Soc. Am. J., 56, 777–783, 1992.

Córdova, S. C., Olk, D. C., Dietzel, R. N., Mueller, K. E., Archontouilis, S. V., and Castellano, M. J.: Plant litter quality affects the accumulation rate, composition, and stability of mineral-associated soil organic matter, Soil Biol. Biochem., 125, 115–124, https://doi.org/10.1016/j.soilbio.2018.07.010, 2018.

Cotrufo, M. F., Wallenstein, M. D., Boot, C. M., Denef, K., and Paul, E.: The Microbial Efficiency-Matrix Stabilization (MEMS) framework integrates plant litter decomposition with soil organic matter stabilization: do labile plant inputs form stable soil organic matter?, Glob Change Biol, 19, 988–995, https://doi.org/10.1111/gcb.12113, 2013.

Cotrufo, M. F., Soong, J. L., Horton, A. J., Campbell, E. E., Haddix, M. L., Wall, D. H., and Parton, W. J.: Formation of soil organic matter via biochemical and physical pathways of litter mass loss, Nature Geosci, 8, 776–779, https://doi.org/10.1038/ngeo2520, 2015.

Crow, S. E., Deem, L. M., Sierra, C. A., and Wells, J. M.: Belowground Carbon Dynamics in Tropical Perennial C4 Grass Agroecosystems, Front. Environ. Sci., 6, 18, https://doi.org/10.3389/fenvs.2018.00018, 2018.

Crow, S. E., Wells, J. M., Sierra, C. A., Youkhana, A. H., Ogoshi, R. M., Richardson, D., Tallamy Glazer, C., Meki, M. N., and Kiniry, J. R.: Carbon flow through energycane agroecosystems established post-intensive agriculture, GCB Bioenergy, 12, 806–817, https://doi.org/10.1111/gcbb.12713, 2020.

Daly, A. B., Jilling, A., Bowles, T. M., Buchkowski, R. W., Frey, S. D., Kallenbach, C. M., Keiluweit, M., Mooshammer, M., Schimel, J. P., and Grandy, A. S.: A holistic framework integrating plant-microbe-mineral regulation of soil bioavailable nitrogen, Biogeochemistry, 154, 211–229, https://doi.org/10.1007/s10533-021-00793-9, 2021.

Davis, A. S., Hill, J. D., Chase, C. A., Johanns, A. M., and Liebman, M.: Increasing Cropping System Diversity Balances Productivity, Profitability and Environmental Health, PLoS One, 7, 8, https://doi.org/10.1371/journal.pone.0047149, 2012.

Díaz, R. and Morón, A. (Eds.): 40 años de Rotaciones Agrícolas-Ganaderas (Serie Técnica 134), INIA, 2003.

570   Fargione, J. E., Bassett, S., Boucher, T., Bridgham, S. D., Conant, R. T., Cook-Patton, S. C., Ellis, P. W., Falcucci, A.,
       Fourqurean, J. W., Gopalakrishna, T., Gu, H., Henderson, B., Hurteau, M. D., Kroeger, K. D., Kroeger, T., Lark, T. J.,
       Leavitt, S. M., Lomax, G., McDonald, R. I., Megonigal, J. P., Miteva, D. A., Richardson, C. J., Sanderman, J., Shoch, D.,
       Spawn, S. A., Veldman, J. W., Williams, C. A., Woodbury, P. B., Zganjar, C., Baranski, M., Elias, P., Houghton, R. A.,
       Landis, E., McGlynn, E., Schlesinger, W. H., Siikamaki, J. V., Sutton-Grier, A. E., and Griscom, B. W.: Natural climate
575   solutions for the United States, Sci. Adv., 4, eaat1869, https://doi.org/10.1126/sciadv.aat1869, 2018.

       Grahmann, K., Rubio Dellepiane, V., Terra, J. A., and Quincke, J. A.: Long-term observations in contrasting crop-pasture
       rotations over half a century: Statistical analysis of chemical soil properties and implications for soil sampling frequency,
       Agric Ecosyst Environ, 287, 106710, https://doi.org/10.1016/j.agee.2019.106710, 2020.

       Grant, C. A., Dribnenki, J. C. P., and Bailey, L. D.: A comparison of the yield response of solin (cv. Linola 947) and flax
580   (cvs. McGregor and Vimy) to application of nitrogen, phosphorus, and Provide (*Penicillium bilaji*), Can. J. Plant Sci., 79,
       527–533, https://doi.org/10.4141/P98-085, 1999.

       Hall, S. J., Russell, A. E., and Moore, A. R.: Do corn-soybean rotations enhance decomposition of soil organic matter?, Plant
       Soil, 444, 427–442, https://doi.org/10.1007/s11104-019-04292-7, 2019.

       Hua, Q., Turnbull, J. C., Santos, G. M., Rakowski, A. Z., Ancapichún, S., De Pol-Holz, R., Hammer, S., Lehman, S. J.,
585   Levin, I., Miller, J. B., Palmer, J. G., and Turney, C. S. M.: Atmospheric radiocarbon for the period 1950–2019, Radiocarbon,
       64, 723–745, https://doi.org/10.1017/RDC.2021.95, 2022.

       INIA GRAS: Unidad de Agro-clima y Sistemas de información (GRAS), 2023.

       IUSS Working Group: World reference base for soil resources 2014, FAO, Rome, 2014.

       Janowiak, M., Connelly, W. J., Dante-Wood, K., Domke, G. M., Giardina, C., Kayler, Z., Marcinkowski, K., Ontl, T.,
590   Rodriguez-Franco, C., Swanston, C., Woodall, C. W., and Buford, M.: Considering Forest and Grassland Carbon in Land
       Management, U.S. Department of Agriculture, Forest Service, Washington Office, Washington, DC,
       https://doi.org/10.2737/WO-GTR-95, 2017.

       Jobbágy, E. G. and Jackson, R. B.: The vertical distribution of soil organic carbon and its relation to climate and vegetation,
       Ecol. Appl., 10, 423–436, https://doi.org/10.1890/1051-0761(2000)010[0423:TVDOSO]2.0.CO;2, 2000.

595   Kallenbach, C. M., Frey, S. D., and Grandy, A. S.: Direct evidence for microbial-derived soil organic matter formation and
       its ecophysiological controls, Nat Commun, 7, 13630, https://doi.org/10.1038/ncomms13630, 2016.

       Kätterer, T. and Andrén, O.: Long-term agricultural field experiments in Northern Europe: analysis of the influence of
       management on soil carbon stocks using the ICBM model, Agric Ecosyst Environ, 72, 165–179,
       https://doi.org/10.1016/S0167-8809(98)00177-7, 1999.

600   Kleber, M., Nico, P. S., Plante, A., Filley, T., Kramer, M., Swanston, C., and Sollins, P.: Old and stable soil organic matter is
       not necessarily chemically recalcitrant: implications for modeling concepts and temperature sensitivity, Glob Chang Biol, 17,
       1097–1107, https://doi.org/10.1111/j.1365-2486.2010.02278.x, 2011.

       Lal, R.: Beyond COP 21: Potential and challenges of the "4 per Thousand" initiative, JSWC, 71, 20A-25A,
       https://doi.org/10.2489/jswc.71.1.20A, 2016.

605   Lal, R.: Digging deeper: A holistic perspective of factors affecting soil organic carbon sequestration in agroecosystems, Glob
       Change Biol, 24, 3285–3301, https://doi.org/10.1111/gcb.14054, 2018.

Lehmann, J. and Kleber, M.: The contentious nature of soil organic matter, Nature, 528, 60–68, https://doi.org/10.1038/nature16069, 2015.

Ma, T., Zhu, S., Wang, Z., Chen, D., Dai, G., Feng, B., Su, X., Hu, H., Li, K., Han, W., Liang, C., Bai, Y., and Feng, X.:
610 Divergent accumulation of microbial necromass and plant lignin components in grassland soils, Nat Commun, 9, 3480, https://doi.org/10.1038/s41467-018-05891-1, 2018.

Makowski, D., Ben-Shachar, M., and Lüdecke, D.: bayestestR: Describing Effects and their Uncertainty, Existence and Significance within the Bayesian Framework, JOSS, 4, 1541, https://doi.org/10.21105/joss.01541, 2019.

Manzoni, S., Katul, G. G., and Porporato, A.: Analysis of soil carbon transit times and age distributions using network
615 theories, J. Geophys. Res., 114, G04025, https://doi.org/10.1029/2009JG001070, 2009.

Mercau, J. L., Dardanelli, J. L., Collino, D. J., Andriani, J. M., Irigoyen, A., and Satorre, E. H.: Predicting on-farm soybean yields in the pampas using CROPGRO-soybean, Field Crops Res., 100, 200–209, https://doi.org/10.1016/j.fcr.2006.07.006, 2007.

Metzler, H. and Sierra, C. A.: Linear Autonomous Compartmental Models as Continuous-Time Markov Chains: Transit-
620 Time and Age Distributions, Math Geosci, 50, 1–34, https://doi.org/10.1007/s11004-017-9690-1, 2018.

Nowinski, N. S., Taneva, L., Trumbore, S. E., and Welker, J. M.: Decomposition of old organic matter as a result of deeper active layers in a snow depth manipulation experiment, Oecologia, 163, 785–792, https://doi.org/10.1007/s00442-009-1556-x, 2010.

Ogle, S. M., Swan, A., and Paustian, K.: No-till management impacts on crop productivity, carbon input and soil carbon
625 sequestration, Agric Ecosyst Environ, 149, 37–49, https://doi.org/10.1016/j.agee.2011.12.010, 2012.

Pausch, J. and Kuzyakov, Y.: Carbon input by roots into the soil: Quantification of rhizodeposition from root to ecosystem scale, Glob Change Biol, 24, 1–12, https://doi.org/10.1111/gcb.13850, 2018.

Pravia, M. V., Kemanian, A. R., Terra, J. A., Shi, Y., Macedo, I., and Goslee, S.: Soil carbon saturation, productivity, and carbon and nitrogen cycling in crop-pasture rotations, Agric. Syst., 171, 13–22, https://doi.org/10.1016/j.agsy.2018.11.001,
630 2019.

Quincke, J., Ciganda, V., Sawchik, J., Fernández, E., Hirigoyen, D., Sotelo, D., Restaino, E., and Lapetina, J.: Rotaciones cultivos pasturas INIA La Estanzuela: Aprendiendo del experimento más antiguo de Latinoamérica, 59, 46–60, 2019.

R Core Team: R: A language and environment for statistical computing, 2023.

Reimer, P. J., Bard, E., Bayliss, A., Beck, J. W., Blackwell, P. G., Ramsey, C. B., Buck, C. E., Cheng, H., Edwards, R. L.,
635 Friedrich, M., Grootes, P. M., Guilderson, T. P., Haflidason, H., Hajdas, I., Hatté, C., Heaton, T. J., Hoffmann, D. L., Hogg, A. G., Hughen, K. A., Kaiser, K. F., Kromer, B., Manning, S. W., Niu, M., Reimer, R. W., Richards, D. A., Scott, E. M., Southon, J. R., Staff, R. A., Turney, C. S. M., and Van Der Plicht, J.: IntCal13 and Marine13 Radiocarbon Age Calibration Curves 0–50,000 Years cal BP, Radiocarbon, 55, 1869–1887, https://doi.org/10.2458/azu_js_rc.55.16947, 2013.

Rui, Y., Jackson, R. D., Cotrufo, M. F., Sanford, G. R., Spiesman, B. J., Deiss, L., Culman, S. W., Liang, C., and Ruark, M.
640 D.: Persistent soil carbon enhanced in Mollisols by well-managed grasslands but not annual grain or dairy forage cropping systems, Proc. Natl. Acad. Sci. U.S.A., 119, e2118931119, https://doi.org/10.1073/pnas.2118931119, 2022.

Schmidt, M. W., Torn, M. S., Abiven, S., Dittmar, T., Guggenberger, G., Janssens, I. A., Kleber, M., Kögel-Knabner, I., Lehmann, J., and Manning, D. A.: Persistence of soil organic matter as an ecosystem property, Nature, 478, 49–56, https://doi.org/10.1038/nature10386, 2011.

645   Sierra, C. A., Müller, M., and Trumbore, S. E.: Models of soil organic matter decomposition: the SoilR package, version 1.0, Geosci. Model Dev., 5, 1045–1060, https://doi.org/10.5194/gmd-5-1045-2012, 2012a.

Sierra, C. A., Trumbore, S. E., Davidson, E. A., Frey, S. D., Savage, K. E., and Hopkins, F. M.: Predicting decadal trends and transient responses of radiocarbon storage and fluxes in a temperate forest soil, Biogeosciences, 9, 3013–3028, https://doi.org/10.5194/bg-9-3013-2012, 2012b.

650   Sierra, C. A., Jiménez, E. M., Reu, B., Peñuela, M. C., Thuille, A., and Quesada, C. A.: Low vertical transfer rates of carbon inferred from radiocarbon analysis in an Amazon Podzol, Biogeosciences, 10, 3455–3464, https://doi.org/10.5194/bg-10-3455-2013, 2013.

Sierra, C. A., Müller, M., and Trumbore, S. E.: Modeling radiocarbon dynamics in soils: SoilR version 1.1, Biogeosciences, https://doi.org/10.5194/gmdd-7-3161-2014, 2014.

655   Sierra, C. A., Müller, M., Metzler, H., Manzoni, S., and Trumbore, S. E.: The muddle of ages, turnover, transit, and residence times in the carbon cycle, Glob Change Biol, 23, 1763–1773, https://doi.org/10.1111/gcb.13556, 2017.

Sierra, C. A., Ceballos-Núñez, V., Metzler, H., and Müller, M.: Representing and Understanding the Carbon Cycle Using the Theory of Compartmental Dynamical Systems, J. Adv. Model. Earth Syst., 10, 1729–1734, https://doi.org/10.1029/2018MS001360, 2018a.

660   Sierra, C. A., Hoyt, A. M., He, Y., and Trumbore, S. E.: Soil Organic Matter Persistence as a Stochastic Process: Age and Transit Time Distributions of Carbon in Soils, Global Biogeochem. Cycles, 32, 1574–1588, https://doi.org/10.1029/2018GB005950, 2018b.

Sierra, C. A., Crow, S. E., Heimann, M., Metzler, H., and Schulze, E.-D.: The climate benefit of carbon sequestration, Biogeosciences, 18, 1029–1048, https://doi.org/10.5194/bg-18-1029-2021, 2021.

665   Soetaert, K. and Petzoldt, T.: Inverse Modelling, Sensitivity and Monte Carlo Analysis in R Using Package FME, J. Stat. Soft., 33, https://doi.org/10.18637/jss.v033.i03, 2010.

Soil Survey Staff: Keys to soil taxonomy, 12th ed., United States Department of Agriculture, Natural Resources Conservation Service, Washington DC, USA., 2014.

Sokol, N. W. and Bradford, M. A.: Microbial formation of stable soil carbon is more efficient from belowground than
670   aboveground input, Nature Geosci, 12, 46–53, https://doi.org/10.1038/s41561-018-0258-6, 2019.

Spohn, M. and Giani, L.: Impacts of land use change on soil aggregation and aggregate stabilizing compounds as dependent on time, Soil Biol. Biochem., 43, 1081–1088, https://doi.org/10.1016/j.soilbio.2011.01.029, 2011.

Spohn, M., Braun, S., and Sierra, C. A.: Continuous decrease in soil organic matter despite increased plant productivity in an 80-years-old phosphorus-addition experiment, Commun Earth Environ, 4, 251, https://doi.org/10.1038/s43247-023-00915-1,
675   2023.

Stoner, S. W., Hoyt, A. M., Trumbore, S., Sierra, C. A., Schrumpf, M., Doetterl, S., Baisden, W. T., and Schipper, L. A.: Soil organic matter turnover rates increase to match increased inputs in grazed grasslands, Biogeochemistry, https://doi.org/10.1007/s10533-021-00838-z, 2021.

680 Tinsley, J.: The determination of organic carbon in soils by dichromate mixtures, Transactions 4th International Congress on Soil Science, 161–164, 1950.

Torn, M. S., Swanston, C. W., Castanha, C., and Trumbore, S. E.: Storage and Turnover of Organic Matter in Soil, in: Biophysico-Chemical Processes Involving Natural Nonliving Organic Matter in Environmental Systems, edited by: Senesi, N., Xing, B., and Huang, P. M., John Wiley & Sons, Inc., Hoboken, NJ, USA, 219–272, https://doi.org/10.1002/9780470494950.ch6, 2009.

685 Torn, M. S., Kleber, M., Zavaleta, E. S., Zhu, B., Field, C. B., and Trumbore, S. E.: A dual isotope approach to isolate soil carbon pools of different turnover times, Biogeosciences, 10, 8067–8081, https://doi.org/10.5194/bg-10-8067-2013, 2013.

Trumbore, S.: Age of Soil Organic Matter and Soil Respiration: Radiocarbon Constraints on Belowground C Dynamics, Ecol. Appl., 10, 399–411, https://doi.org/10.1890/1051-0761(2000)010[0399:AOSOMA]2.0.CO;2, 2000.

Trumbore, S.: Radiocarbon and Soil Carbon Dynamics, Annu. Rev. Earth Planet. Sci., 37, 47–66,
690 https://doi.org/10.1146/annurev.earth.36.031207.124300, 2009.

Trumbore, S. E., Xu, X., Santos, G. M., Czimczik, C. I., Beaupré, S. R., Pack, M. A., Hopkins, F. M., Stills, A., Lupascu, M., and Ziolkowski, L.: Preparation for Radiocarbon Analysis, edited by: Schuur, E. A. G., Druffel, E., and Trumbore, S. E., Radiocarbon and Climate Change: Mechanisms, Applications and Laboratory Techniques, 279–315, 2016a.

Trumbore, S. E., Sierra, C. A., and Hicks Pries, C. E.: Radiocarbon Nomenclature, Theory, Models, and Interpretation:
695 Measuring Age, Determining Cycling Rates, and Tracing Source Pools, in: Radiocarbon and Climate Change, edited by: Schuur, E. A. G., Druffel, E., and Trumbore, S. E., Springer International Publishing, 45–82, 2016b.

Unkovich, M., Baldock, J., and Forbes, M.: Variability in Harvest Index of Grain Crops and Potential Significance for Carbon Accounting: Examples from Australian Agriculture, Adv. Agron, 105, 173–219, https://doi.org/10.1016/S0065-2113(10)05005-4, 2010.

700 Villarino, S. H., Pinto, P., Jackson, R. B., and Piñeiro, G.: Plant rhizodeposition: A key factor for soil organic matter formation in stable fractions, Sci. Adv., 7, 3176, https://doi.org/10.1126/sciadv.abd3176, 2021.

Wright, A. F. and Bailey, J. S.: Organic carbon, total carbon, and total nitrogen determinations in soils of variable calcium carbonate contents using a Leco CN-2000 dry combustion analyzer, Commun Soil Sci Plant Anal, 32, 3243–3258, https://doi.org/10.1081/CSS-120001118, 2001.

705 Zhu, X., Jackson, R. D., DeLucia, E. H., Tiedje, J. M., and Liang, C.: The soil microbial carbon pump: From conceptual insights to empirical assessments, Glob Chang Biol, 26, 6032–6039, https://doi.org/10.1111/gcb.15319, 2020.